GW182 is critical for the stability of GW bodies expressed during the cell cycle and cell proliferation

Zheng Yang[1,*,‡], Andrew Jakymiw[1,*], Malcolm R. Wood[2], Theophany Eystathioy[3], Robert L. Rubin[4], Marvin J. Fritzler[3] and Edward K. L. Chan[1,§]

[1]Department of Oral Biology, University of Florida, PO Box 100424, Gainesville, FL 32610-0424, USA
[2]The Core Microscopy Facility, The Scripps Research Institute, 10550 North Torrey Pines Road, La Jolla, CA 92037, USA
[3]Department of Biochemistry and Molecular Biology, University of Calgary, 3330 Hospital Drive, Calgary, Alberta, T2N 4N1, Canada
[4]Department of Molecular Genetics and Microbiology, University of New Mexico School of Medicine, 915 Camino de Salud NE, Albuquerque, NM 87131, USA

*Authors contributed equally to this work
‡Present address: Department of Medicine, School of Medicine, University of California at San Diego, La Jolla, CA 92093, USA
§Author for correspondence (e-mail: echan@ufl.edu)

Accepted 2 August 2004
Journal of Cell Science 117, 5567-5578 Published by The Company of Biologists 2004
doi:10.1242/jcs.01477

Summary

A novel cytoplasmic compartment referred to as GW bodies was initially identified using human autoantibodies to a 182 kDa protein named GW182. GW bodies are small, generally spherical, cytoplasmic domains that vary in number and size in several mammalian cell types examined to date. Based on our earlier studies, GW bodies were proposed to be cytoplasmic sites for mRNA storage and/or degradation. In the present study, immunogold electron microscopy identified electron dense structures of 100-300 nm diameter devoid of a lipid bilayer membrane. These structures appeared to comprise clusters of electron dense strands of 8-10 nm in diameter. By costaining with CENP-F and PCNA, and employing a double-thymidine block to synchronize HeLa cells, GW bodies were observed to be small in early S phase and larger during late S and G2 phases of the cell cycle. The majority of GW bodies disassembled prior to mitosis and small GW bodies reassembled in early G1. The analysis of GW bodies in two experimental models of cell proliferation using reversal of 3T3/serum-starvation and concanavalin A stimulation of mouse splenocytes and T cells, revealed that proliferating cells contained larger, brighter, and more numerous GW bodies as well as up to a fivefold more total GW182 protein than quiescent cells. In vitro gene knockdown of GW182 led to the disappearance of GW bodies demonstrating that GW182 is a critical component of GW bodies. The incremental expression of the GW182 protein in cells induced to proliferate and the cyclic formation and breakdown of GW bodies during mitosis are intriguing in view of the notion that GW bodies are specialized centers involved in maintaining stability and/or controlling degradation of mRNA.

http://jcs.biologists.org/cgi/content/full/117/23/5567/DC1

Key words: mRNA degradation complex, GW repeats, GW bodies

Introduction

In 2002, we reported the identification and cloning of a novel 182 kDa protein named GW182, which we isolated using a patient serum to immunoscreen a HeLa cDNA library (Eystathioy et al., 2002a). GW182 contains multiple glycine/tryptophan (GW) repeats and a classic RNA-binding domain (or RNA recognition motif, RRM) near the C terminus. GW182 appears to react with a subset of mRNAs and localizes to discrete cytoplasmic domains that do not colocalize to any of the known conventional organelles in the cytoplasm (Eystathioy et al., 2002a). Hence, we tentatively identified the cytoplasmic domain marked by antibodies directed against GW182 as GW bodies or GWBs. The mRNAs associated with GW182 represent a clustered set of transcripts that are presumed to reside within GWBs. We proposed that the GW182 ribonucleoprotein complex is involved in the post-transcriptional regulation of gene expression by sequestering a specific subset of gene transcripts involved in cell growth and homeostasis. Epitopes bound by the human autoantibodies were mapped to the GW-rich mid-part of the protein, the non-GW rich region, and the C-terminus of GW182 protein (Eystathioy et al., 2003a; Eystathioy et al., 2003b). None of the GW182 epitopes or the GW182 protein itself had significant sequence similarities to other known proteins.

Until recently, the dogma for gene regulation was that most genes are expressed and regulated primarily at the transcriptional level and that transcriptional regulation generally operates at the level of individual genes. The important components involved in this regulation include the gene promoter, enhancer elements and the binding of transcription factors, co-activators and RNA polymerases required for the initiation of transcription. Much of this dogma was deduced from in vitro experiments using DNA plasmid templates, purified factors and RNA polymerase complexes, cell transfection and transgenic animals. Recent studies have raised some serious concerns for this classical model of gene regulation. An important study by Spellman and Rubin (Spellman and Rubin, 2002) showed, by determining gene-expression profiles of over 80 experimental conditions, that gene expression actually occurs in groups of adjacent genes

that are not otherwise functionally related in any obvious way; these groups span 20 to 200 kilobase pairs of genomic sequence. This finding that neighboring eukaryotic genes are often expressed in similar patterns suggests that 'chromatin domains' are involved in the control of genes within a genomic neighborhood (Oliver et al., 2002). This also suggests that transcriptional regulation at the individual gene level is clearly not as highly regulated as previously considered and that regulation of gene expression at other levels must occur. Independent of the discovery of gene expression neighborhoods as discussed above, once transcription generates mRNA, the next level of gene expression regulation is likely to take place at the mRNA level including mRNA transport, storage and degradation (Keene, 2003).

Recently, discrete cytoplasmic foci that contained hLSm complex proteins 1-7, as well as the hDcp1 protein were described and, interestingly, cytoplasmic foci containing these proteins resembled GWBs (Ingelfinger et al., 2002; Van Dijk et al., 2002). Both the hLSm1-7 complex (Tharun et al., 2000; Bouveret et al., 2000; Tharun and Parker, 2001) and hDcp (Dunckley and Parker, 1999; Dunckley and Parker, 2001; Van Dijk et al., 2002) are believed to be involved in mRNA decapping and other processes of mRNA degradation. In mammalian cells, decapping has been suggested to be an important step in the process of mRNA decay (Couttet et al., 1997; Gao et al., 2001). Taken together, these observations suggest that the GW182 protein and GWBs are involved in mRNA metabolism and more specifically GWBs may be functional sites within the cytoplasm involved in the degradation of specific mRNAs. Recently we demonstrated that the hLSm4 protein, a component of the hLSm1-7 complex, and the hDcp1 protein co-localize with GW182 in GWBs and this supported the hypothesis that GWBs are involved in mRNA degradation (Eystathioy et al., 2003c).

When we first identified GWBs by indirect immunofluorescence (IIF), it appeared that there were cell-cycle-dependent variations in expression because not all cells had the same number or size of GWBs. We have now characterized the expression of GW182 and GWBs during the cell cycle and proliferation and show that GW182 expression plays an important role in the stability of GWBs.

Materials and Methods

Antibodies

Human sera used in this study were obtained from a serum bank at the Advanced Diagnostics Laboratory, University of Calgary, Canada. The index human anti-GW182 serum was obtained from a Caucasian female with a severe mixed motor and sensory polyneuropathy. The selection of this serum was based on its unique reactivity to an apparently novel cytoplasmic domain (Eystathioy et al., 2002a). A second human anti-GW182 serum IC6, known to have additional nuclear envelope antibodies (Ou et al., 2004) was used in some experiments to demonstrate the specificity of the GW182 siRNA construct. Rabbit anti-GW182 (Eystathioy et al., 2002a) and mouse monoclonal antibodies to GW182 (Eystathioy et al., 2003a), rabbit anti-LSm4 (Eystathioy et al., 2002b), mouse monoclonal antibody 72B9 to fibrillarin (Reimer et al., 1987) and rabbit anti-CENP-F (centromere protein F) (Casiano et al., 1993; Casiano et al., 1995) were generated as previously described. Specific human anti-PCNA (proliferating cell nuclear antigen) serum was kindly provided by Dr Yoshinari Takasaki, Juntendo University, Tokyo, Japan (Takasaki et al., 1984). Mouse monoclonal anti-tubulin was purchased from Sigma-Aldrich (St Louis, MO, USA).

Double thymidine block of HeLa cells at S phase

HeLa S3 cells (American Type Culture Collection, Rockville, MD, USA) were grown in Dulbecco's modified Eagle's medium (DMEM; Invitrogen Corporation, Carlsbad, CA, USA) containing 10% fetal bovine serum (FBS; Omega Scientific, Inc., Tarzana, CA, USA). Cells were arrested at S phase using the double thymidine block method (Bootsma et al., 1964). In brief, cells were cultured for 3 days to logarithmic phase and then incubated in medium containing 3.5 mM thymidine (Sigma-Aldrich) for 24 hours. Cells were then washed twice with tissue culture grade PBS, and incubated with regular medium for 18 hours before a second incubation in 3.5 mM thymidine for 24 hours. Cells were analyzed by indirect immunofluorescence (IIF) and western blotting at 0, 3, 6 and 9 hours after release from the second thymidine block.

Serum starvation as a model for cell proliferation analysis

Mouse fibroblast 3T3 cells (ATCC) were maintained in DMEM culture medium supplemented with 10% FBS. Serum starvation experiments were performed as previously described (Andrade et al., 1993). In brief, cells were placed in DMEM containing 0.1% FBS for 72 hours. After refeeding with medium containing 10% fetal bovine serum (FBS), cells were collected every 3 hours up to 24 hours for analysis by IIF and western blotting. The quality of synchronization of quiescent cells during serum starvation and the percentage of proliferating cells after refeeding was monitored by staining with PCNA, a known marker of cell proliferation.

Concanavalin A stimulated cell proliferation of mouse splenocytes and isolated T cells

Mouse splenocytes were isolated from B10.BR/SgSnJ mice. For some experiments T cells were enriched by passage through nylon wool fiber columns (Polysciences, Inc., Warrington, PA, USA) using standard procedures (Mishell and Shiigi, 1980) and the manufacturer's instructions. Cells were cultured in RPMI 1640 medium supplemented with 10% FBS and 50 μM β-mercaptoethanol, 20 mM Hepes, 100 μM non-essential amino acids, 1 mM pyruvate, 50 μg/ml gentamycin and 0.5 μg/ml fungizone. 5×10^6 splenocytes or 2×10^6 T cells mixed with 500,000 3000R-irradiated splenocytes were cultured in 2 ml of supplemented medium in 6-well plates in the presence or absence of 5 μg/ml concanavalin A (ConA) and harvested after 2, 3 or 4 days for IIF and western blot analysis.

Preparation of cell extract and western blotting

Cells were trypsinized at various time points and washed twice in ice-cold PBS. Two volumes of lysis buffer A (10 mM Tris, pH 7.5, 150 mM NaCl, 1.5 mM $MgCl_2$ and 1% NP-40) with complete EDTA-free protease inhibitor (Roche, Palo Alto, CA, USA) were added to 1 volume of cell pellet, mixed and placed on ice for 10 minutes. The resulting lysate was centrifuged at 12,000 ***g*** for 15 minutes in a cold room. The soluble (supernatant) and insoluble (pellet) fractions were separated. Both fractions were analyzed on a 5% SDS-polyacrylamide gel and transferred to nitrocellulose. The nitrocellulose membrane was blocked in 5% nonfat dried milk in PBST for 30 minutes, and then probed with the index human anti-GW182 serum (1:500 dilution) for 1 hour at room temperature, followed by incubation with horseradish peroxidase-conjugated goat anti-human IgG (Caltag, Burlingame, CA, USA) for 1 hour at room temperature. Immunoreactive bands were detected by the SuperSignal chemiluminescence system (Pierce, Rockford, IL, USA) according to the manufacturer's instructions.

DNA constructs and cell transfection

Plasmids expressing the GFP-GW182 construct were described and characterized in an earlier report (Eystathioy et al., 2002a). Short hairpin RNA (shRNA) plasmid constructs designed to specifically knockdown the GW182 gene were constructed into the pSHAG vector, with the aid of the software program RNA Oligo Retriever (Paddison et al., 2002). Primer pairs were designed to target GW182 nucleotide position 721 and 1570 respectively; position 721: GAAGTGCCATTCATACCTGATGGAGCCTGAAGCTTGAGGCTCCGTCGGGTATGAATGGTACTTCTCTTTTTTT and GATCAAAAAAAGAGAAGTACCATTCATACCCGACGGAGCCTCAAGCTTCAGGCTCCATCAGGTATGAATGGCACTTCCG; position 1570: GGATCGCCCCACCCTGATACAGATGAGGGAAGCTTGCTTCGTCTGTGTCGGGGTGGGGCGATCCCAATTTTTT and GATCAAAAAATTGGGATCGCCCCACCCCGACACAGACGAAGCAAGCTTCCCTCATCTGTATCAGGGTGGGGCGATCCCG. These oligonucleotide primers were synthesized by MWG Biotech Inc (High Point, NC, USA). The complementary oligonucleotides were annealed and subsequently cloned into the *Bam*HI and *Bse*RI restriction sites of pSHAG. Constructs were verified by DNA sequencing.

For the initial assay of the functionality of the shRNA construct, HeLa cells were seeded onto 8-chamber slides at ~50,000 cells per well and allowed to attach and cultured at 37°C, 5% CO_2 to ~90% confluency. Transfection of the shRNA construct was carried out using Lipofectamine 2000 (Invitrogen) according to the manufacturer's recommendation. The efficiency of transfection and identification of transfected cells was monitored by a CMV-promoter-driven plasmid phrGFP (Stratagene, La Jolla, CA, USA), which encoded a humanized recombinant green florescent protein that was mixed in 1:6 molar amounts with the shRNA plasmid for transfection. The effects of siRNA on GW182 and GWB expression were monitored after 72 hours of transfection by immunostaining.

Selection of stable cell lines

Prior to transfection, the shRNA plasmid construct (p721) and the plasmid pcDNA3.1(+) (Invitrogen) were linearized by *Not*I and *Sna*BI restriction enzymes, respectively. HeLa cells were then seeded onto a 6-well plate and cultured at 37°C, 5% CO_2 to ~90% confluency. The pcDNA3.1(+) and shRNA constructs were mixed in 1:10 molar amounts, respectively and the transfections were then carried out using Lipofectamine 2000 as stated above. Cells were cultured for 2 days without the selection agent and then selected for 2 months with G418 (Sigma-Aldrich) at 600 μg/ml. Selected cells were cloned and analyzed by western blotting and IIF.

Fluorescence microscopy

Adherent HeLa and HEp-2 cells were grown on 8-chamber slides. Mouse splenocytes and isolated T cells were sedimented onto glass slides with a cytocentrifuge (Shandon, London, UK). The cells were fixed in acetone and methanol 3:1 (vol:vol) at –20°C for 2 minutes. In the siRNA experiment, transfected cells were fixed in 3% paraformaldehyde at room temperature for 10 minutes and permeabilized with 0.5% Triton X-100 at room temperature for 5 minutes. For colocalization studies, the index human anti-GW182 serum (1:500) double stained with rabbit anti-CENP-F (1:200), rabbit anti-LSm4 (1:500), or mouse monoclonal anti-fibrillarin 72B9, cells were incubated at room temperature for 1 hour. After washing with PBS, cells were incubated with corresponding secondary fluorochrome-conjugated antibodies at room temperature for 1 hour. Unless otherwise stated, Alexa Fluro 488 and 568 were the primary fluorochromes used. The nuclei of cells were counterstained with DAPI (4′,6-diamidino-2-phenylindole) dissolved in Vectashield mounting medium (Vector Laboratories, Burlingame, CA, USA). For cell cycle and cell proliferation studies, cells were incubated with either the index human anti-GWB serum (1:200) or human anti-PCNA serum (1:200) using the above-stated protocol. Most fluorescence images were obtained using a Zeiss Axiovert 200M microscope. Excitation wavelengths and filter-sets for GFP, Alexa Fluro 488, Alexa Fluro 568 and DAPI were as supplied by the manufacturer. Images of fixed cells were taken using 63× 1.4 NA or 40× 1.4 NA objectives. Live-cell images were collected on a DeltaVision Deconvolution Restoration Microscope system running SoftWoRx v.2.5 (Applied Precision Inc., Issaquah, WA, USA). The system was mounted on an Olympus IX70 inverted microscope and single-color fluorescent images and differential interference contrast images were captured with a ×100 objective and an auxiliary magnification of ×1.5. Live cells were held at ~30-37°C.

Immunogold electron microscopy (IEM)

HeLa S3 cells were grown in log phase, removed from the flask by gentle scraping and processed according to the method of Raposo et al. (Raposo et al., 1996). The cells were fixed for 1.5 hours in ice-cold 4% paraformaldehyde and 0.025% glutaraldehyde in 0.1 M phosphate buffer, pH 7.4. Following fixation, free aldehydes were quenched in 50 mM glycine in 0.1 M phosphate buffer. The cells were then resuspended in warm 7.5% gelatin in PBS in microfuge tubes for 10 minutes and then pelleted at 10,000 rpm for 1 minute. The tubes were placed on ice and the solidified gelatin pellets were removed, transferred to an ice-cold 50 mM glycine solution, cut into small cubes, and then transferred to 2.3 M sucrose in 0.1 M phosphate buffer at 4°C until clear. Each block of tissue was placed on a cryo pin-head, excess sucrose solution was removed and the pin was immersed and stored in liquid nitrogen. Thin sections (~100 nm) were cut using glass knives and picked up in wire loops dipped in a mixture of methylcellulose and sucrose. The sections were placed directly onto carbon-coated 200 mesh nickel grids. Each grid was processed on individual droplets with the following solutions at room temperature: 50 mM glycine, 10% FBS in PBS, anti-GW182 serum diluted 1/400 in 10% FBS, washed in 0.2% FBS, incubated in protein A tagged with 10 nm gold (Dr J. Slot, University of Utrecht, The Netherlands), washed in PBS, fixed in 1% glutaraldehyde in PBS, washed in double-distilled H_2O and contrasted in uranyl oxalate (pH 7). Individual grids were then picked up in an ice-cold uranyl acetate/methyl cellulose (pH 4) mixture using copper wire loops that were then blotted with filter paper to remove excess solution. The grids were then allowed to dry overnight before examination using a Philips CM-100 transmission electron microscope. Controls included normal incubation with protein A gold alone, normal human serum and rabbit antibodies to the Golgi protein, giantin (Linstedt and Hauri, 1993).

Image analysis

For 8-bit color images, pixel intensity levels were adjusted using Adobe Photoshop so that maximal and minimal values were 0 and 255 in each channel. In movies 1 and 2, the contrast of original images was in some cases increased. Movies employed the Cinepak compression algorithm and were produced using Adobe Premiere.

Results

GWBs are distinct cytoplasmic entities with their number and size varying during the cell cycle

Cytoplasmic GWBs were first observed by IIF on HEp-2 and HeLa cells by using the index human autoimmune serum. Fig. 1A shows a representative image of the cytoplasmic domains in asynchronous cultured HEp-2 cells. In some cells there were more strongly stained structures (arrowheads) than in other cells. To address whether this variation is associated with the cell cycle, we first performed costaining with conventional

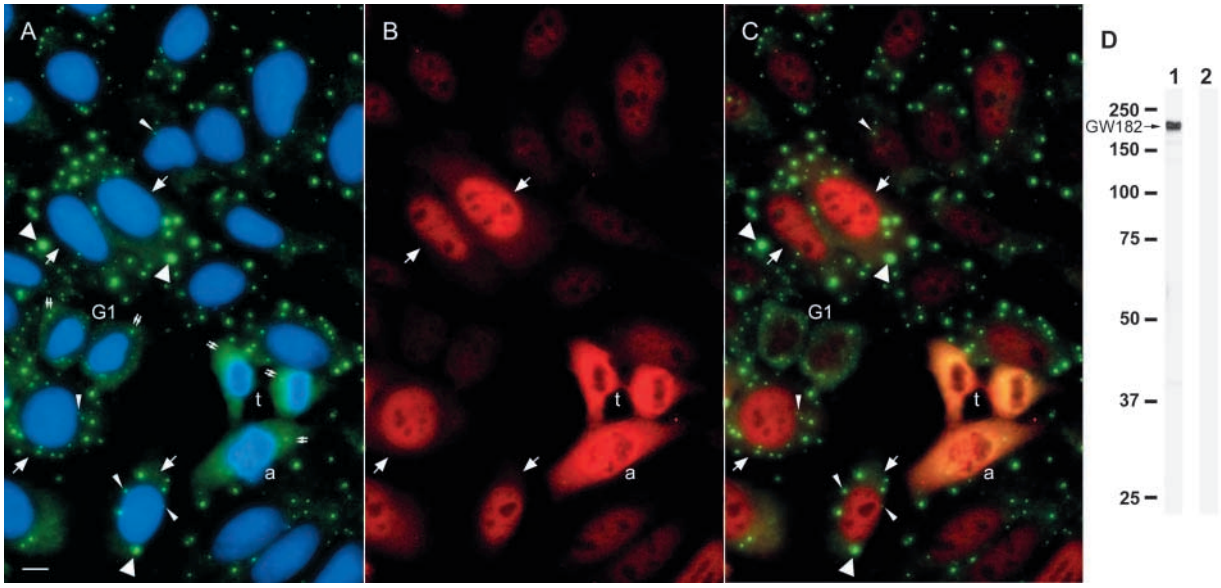

Fig. 1. The number and size of GWBs varies during the cell cycle. (A-C) HEp-2 cells were co-stained with the index human anti-GW182 serum (A, green; nuclei counterstained with DAPI, blue) and rabbit anti-CENP-F antibody (B, red). CENP-F is known to be expressed predominantly in cells in late S or G2 phase and throughout mitosis (B, arrows). (C) The merged image of GW182 and CENP-F. GWBs show cell-cycle-dependent expression, with the largest bodies (arrowheads) detected primarily within cells in the late S or G2 phase. The number of GWBs also is higher in cells with the strongest expression of CENP-F. Staining of GW182 in cells at anaphase (a), telophase (t), and G1 stages are indicated by double-arrows (A). GWBs are sometimes observed adjacent to the nuclear membrane (thin arrowheads). Scale bar: 10 μm. (D) Western blot analysis of the index human anti-GW182 serum (lane 1) and a control normal human serum (lane 2) using HEp-2 cell lysates, separated by SDS-PAGE using a 12.5% gel and transferred to a nitrocellulose membrane.

markers of the cell cycle that were readily available to us, including CENP-F (Fig. 1B,C) and PCNA (data not shown). The level of CENP-F is known to be elevated primarily in late S and G2 phases of the cell cycle as well as throughout mitosis, but is low or absent in G1 and early S phase cells (Rattner et al., 1993; Liao et al., 1995). In the G1 and early S phase cells, GWBs were either present as weak fine speckles or were not detected at all. In contrast to this, interphase cells that stained with CENP-F, indicative of late S and G2 phase, had many GWBs, including the large ones (Fig. 1C, arrowheads). In mitotic cells, GWBs were often not detected and instead the staining appeared diffuse throughout the cells. These observations were consistent among five samples of human anti-GW182 sera in similar costaining experiments with the rabbit anti-CENP-F. Fig. 1D shows the specificity of the index serum indicating that the primary reactivity is to the protein GW182.

GWBs are distinct cytoplasmic clusters of electron dense fibrils of 8 to 10 nm diameter

Using IEM on ultrathin cryosections of HeLa cells, antibodies to GW182 labeled electron dense cytoplasmic bodies that ranged in size from 100 to 300 nm and were not bound by a bilayer lipid membrane. This morphological appearance was quite distinct from other organelles such as mitochondria, endosomes/lysosomes and the Golgi complex. A composite of five selected GWB structures from different cells (Fig. 2) illustrates the variation of the size of GWBs and is consistent with the observations described above when IIF was used. Most of the gold particles were observed on clusters of electron dense fibrils or strands such as those indicated by the arrowheads in Fig. 2A,B,D,E. These fibrils range in diameter from 8 to 10 nm and appear to form the matrix where the gold labels aggregate (for example, arrowheads in Fig. 2E). Some gold labels are observed in the periphery of the cluster (arrows in Fig. 2A,C) while the majority of the gold labels are found clearly within the center of these structures.

Some GWBs are detected adjacent to nuclear envelope

IIF analysis showed that a few GWBs are located adjacent to the nuclear envelope (Fig. 1, thin arrowheads). Fig. 3 illustrates two clusters of gold particles (arrows, Fig. 3A) adjacent to the cytoplasmic face of the nuclear envelope. Note that the locations of these clusters are a short distance from the nuclear pore complexes (arrowheads). Fig. 3B shows the enlarged image of the cluster on the left sitting on the cytoplasmic face of the nuclear envelope. The gold labels decorated an organized structure with electron-dense strands similar to those observed in some of the examples shown in Fig. 2. Fig. 3C shows the enlarged image of the second cluster and it is noted that although the gold particles appear on relatively less electron dense material, the gold clearly labels electron dense strands. Among all the images collected, no GWB-like structures were observed immediately next to nuclear pores and no GWBs were observed on the nuclear face of the inner leaflet of the nuclear envelope.

GWBs disassemble during mitosis

Based on data from asynchronous cell cultures, such as those

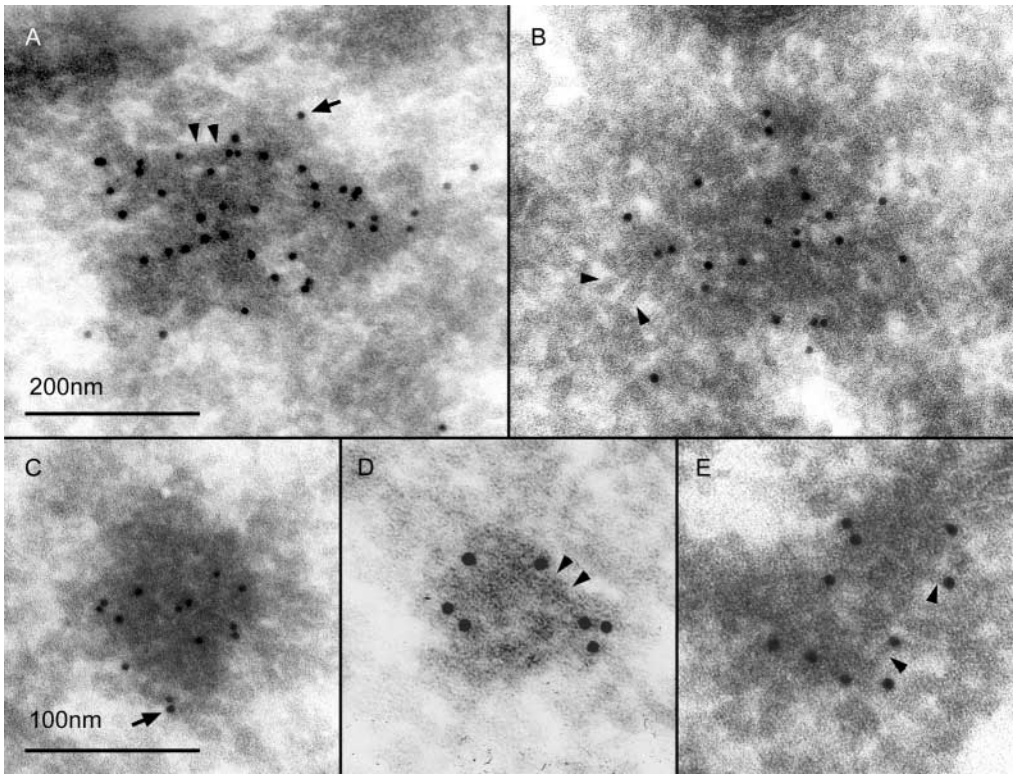

Fig. 2. Immunogold electron microscopy localization of GWBs in the cytoplasm of HeLa cells during interphase. Frozen sections of fixed and gelatin-embedded HeLa cells were incubated with the index human anti-GW182 serum diluted 1:400 and then post-immunolabeled with protein A-gold (10 nm). (A-E) Representative gold-labeled cytoplasmic structures with diameters which vary from 100-300 nm. The gold labels are clustered on electron dense fibrils or strands, 8 to 10 nm in diameter, which are more obvious in some images (arrowheads in A,B,D,E). These fibrils appear to form the matrix that the gold decorates. Some gold particles are observed on the periphery of the cluster (arrows in A,C) while the majority of the gold is found clearly within the center of these structures.

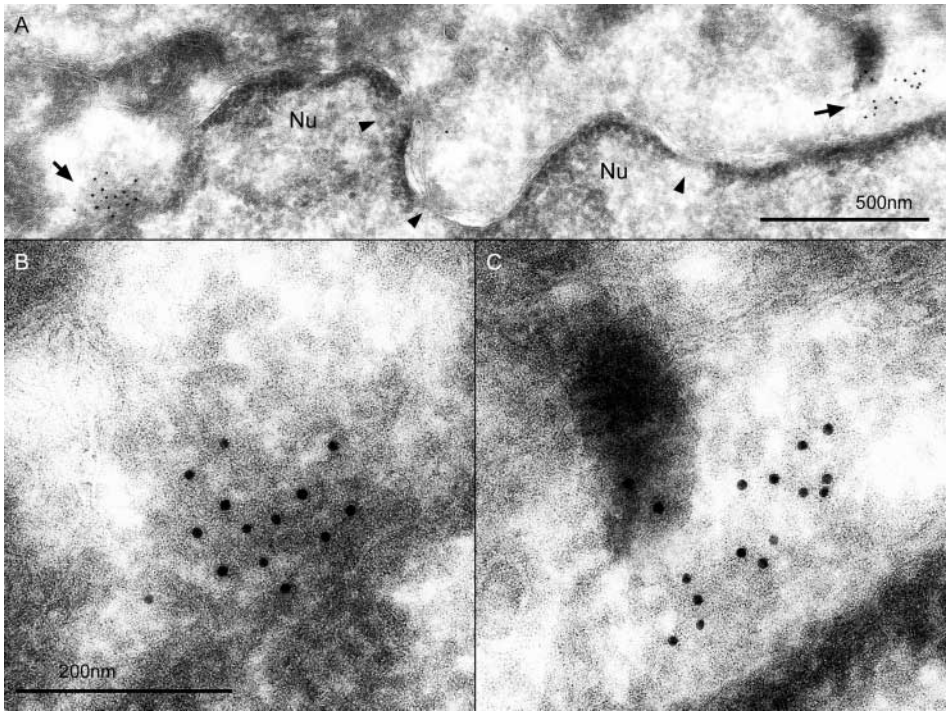

Fig. 3. Immunogold electron microscopy localization of GWBs adjacent to the nuclear membrane in HeLa cells during interphase. (A) Two clusters of gold particles (arrows) adjacent to the cytoplasmic face of the nuclear envelope. Note that they are some distance from nuclear pores (arrowheads). The enlarged images of the two clusters are shown in B and C.

shown in Fig. 1, it appears that a majority of GWBs disassemble before entry into mitosis, but reappear in G1 cells (double arrows in Fig. 1A). Fig. 4 shows composite images of representative cells, at different stages of mitosis, that were double stained for GW182 and the nucleolar protein fibrillarin, a highly conserved 34 kDa marker protein of the U3-snoRNA ribonucleoprotein complex. The nucleolus was used as a reference organelle because it is well known that the nucleolus is disassembled prior to mitosis and reassembles in early G1 cells and thus costaining with fibrillarin can help determine whether there is any spatial relationship in the reassembly of GWBs and the nucleolus. Fig. 4A-D shows that cells in anaphase had no GBWs or nucleoli. In early telophase (Fig. 4E-H), the early reformation

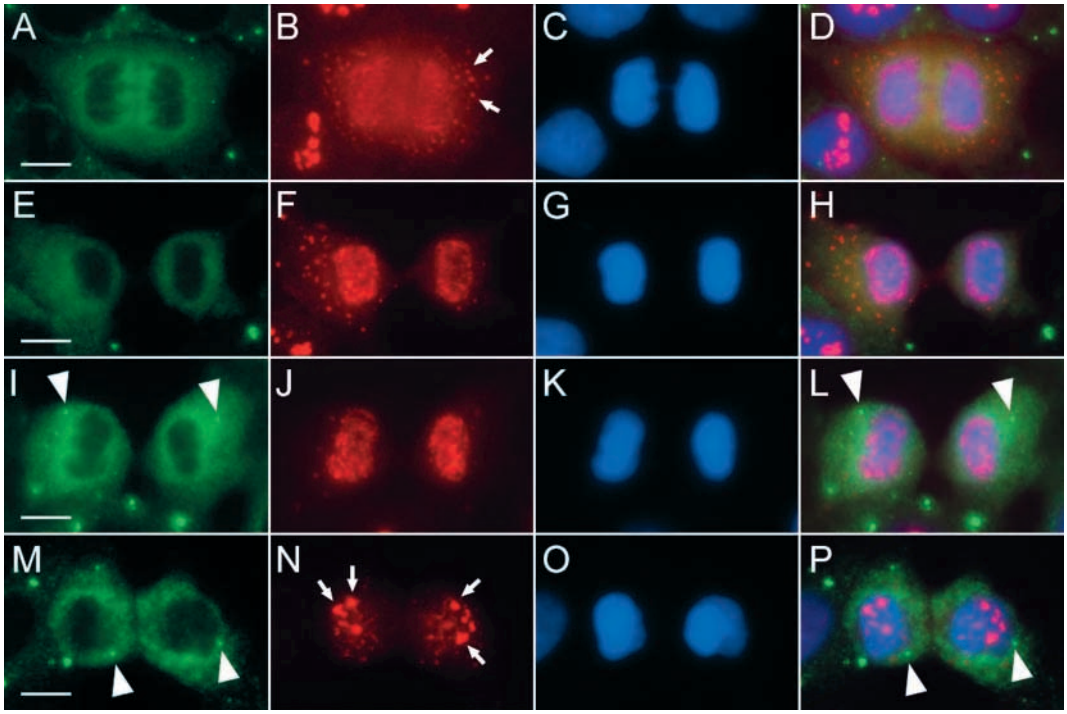

Fig. 4. Disassembly of GWBs before mitosis and reassembly after mitosis was preceded by the reassembly of the nucleolus. HEp-2 cells were double stained with the index human anti-GW182 serum (green, A,E,I,M) and mouse monoclonal anti-fibrillarin antibody 72B9 (red, B,F,J,N). (C,G,K,O) DAPI counterstain; (D,H,L,P) merged images. Cells in anaphase (A-D) or telophase (E-P) show few or no GWBs while diffuse cytoplasmic staining is still visible (A,E). In daughter cells showing maturing nucleoli (I-L, M-P), newly assembled GWBs (arrowheads) are observed. Arrows indicate pre-nucleolar bodies in B and reassembling nucleoli in N.

of nucleoli had begun but GWBs were not detected. Newly formed small GWBs were not seen until the later stage of telophase (Fig. 4I-P), when more mature nucleoli were also detectable (Fig. 4J,N). Therefore, these results demonstrate that the formation of GWBs was preceded by the reassembly of the nucleolus.

Analysis of mitotic cells also showed that the 100-300 nm GWBs were not detected by IEM, a finding largely consistent with the IIF data. However, smaller structures labeled with multiple gold particles were detected in close proximity to the mitotic chromosomes (Fig. 5, arrows). These mitotic 'GWBs' were ~50 nm in diameter, suggesting that some GW182-

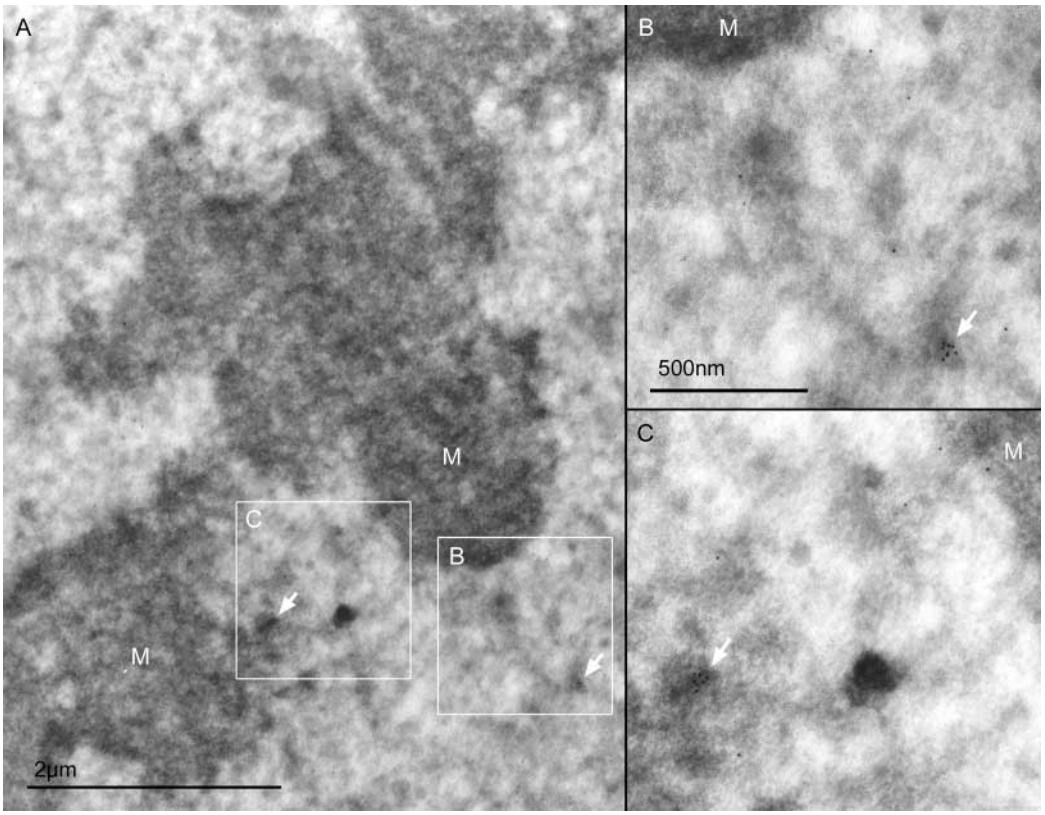

Fig. 5. Immunogold electron microscope images of GWBs in mitotic HeLa cells. Samples were prepared and processed as in Fig. 2. (A) Low magnification of mitotic chromosomes (M). (B,C) Higher magnification views of the boxed areas indicated in A. Arrows show clusters of gold particles adjacent to a mitotic chromosome.

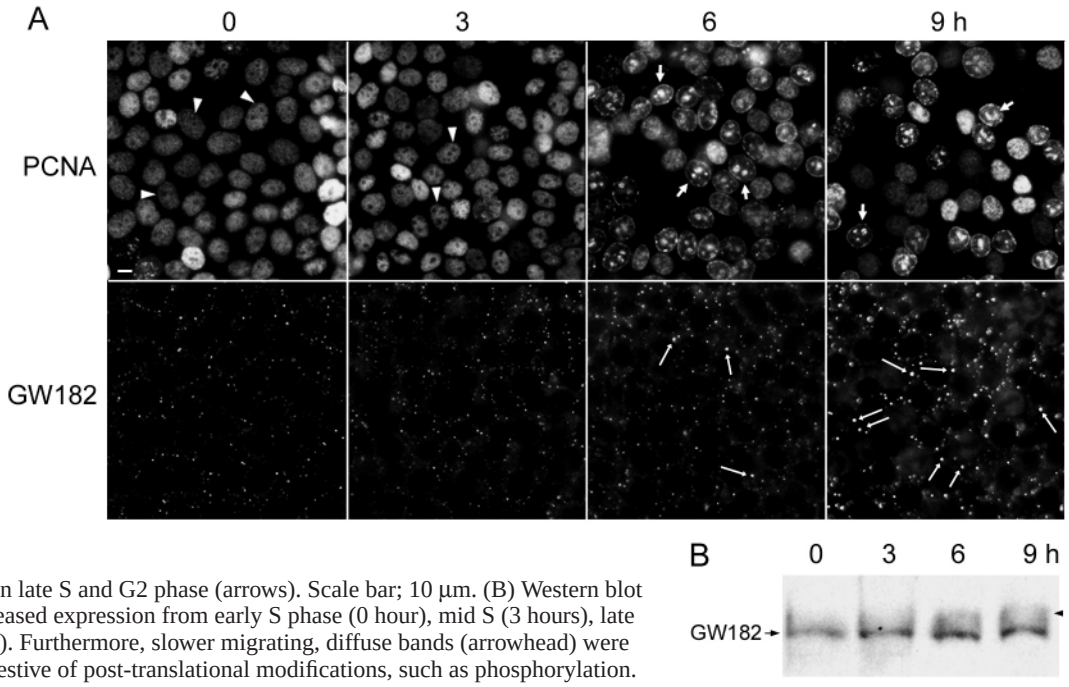

Fig. 6. Expression of GW182 in HeLa cells synchronized by double thymidine block. (A) Cells were processed for IIF at 0, 3, 6 and 9 hours after release from thymidine block and stained with human anti-PCNA serum or the index human anti-GW182 serum. At 0 and 3 hours, most cells stained with anti-PCNA showed the fine nuclear speckled distribution (arrowheads) characteristic of cells in early and mid S phase. Most cells had small GWBs. At 6 and 9 hours, apparently larger GWBs (long arrows) were observed along with the characteristic nucleolar distribution of PCNA in late S and G2 phase (arrows). Scale bar; 10 μm. (B) Western blot analysis of GW182 showed increased expression from early S phase (0 hour), mid S (3 hours), late S (6 hours) to G2 phase (9 hours). Furthermore, slower migrating, diffuse bands (arrowhead) were observed at the later stages suggestive of post-translational modifications, such as phosphorylation.

associated structures might not completely disassemble during mitosis.

Expression of GW182 in HeLa cells synchronized by double thymidine block

The colocalization of GW182 with CENP-F shown in Fig. 1 suggested that smaller GWBs were present in G1/S phase while larger GWBs were present in late S/G2 phase. To further examine the hypothesis that the size of GWBs was related to the cell cycle, we analyzed the expression pattern of GWBs in synchronized cells using the classic thymidine block and release strategy. After double thymidine block as described in the Materials and Methods, HeLa cells were synchronized at S phase, then released from thymidine and examined by IIF and western blot analysis. HeLa cells were immunostained with anti-PCNA to monitor the efficiency of the cell synchronization steps. In early to mid S phase, PCNA is detected as fine nuclear speckles excluding the nucleolus, whereas during late S and G2 phase of the cell cycle its localization changes to the nucleolus (Bravo and Macdonald-Bravo, 1987). Using the characteristic PCNA staining as a monitor of the quality of cell synchronization, our observations indicated that >90% of cells were in S phase after double thymidine block and that the cell synchronization was efficient throughout the procedure (Fig. 6A). GWB staining identified smaller GWBs in early stages, while larger GWBs appeared in the later stages of the cell cycle, consistent with the hypothesis that the expression of GWBs is cell cycle dependent. Cells were harvested and lysed in buffer A at different time points after the cells were released from thymidine block. Both supernatant and pellet fractions were separated by 5% gel SDS-PAGE, after which the proteins were transferred to nitrocellulose and then western blotted with the index human anti-GW182 serum. There was no reactivity in pellet fractions at any of the time points analyzed suggesting that buffer A, containing 1% NP-40, solubilized the majority of GW182 (data not shown). Fig. 6B shows the western blot analysis of GW182 demonstrating increased expression from early S phase (0 hour), mid S (3 hours), late S (6 hours) to G2 phase (9 hours). It was noted that slower migrating, diffuse bands were observed at 6 and 9 hours after release from thymidine block. This pattern of expression at the later stage of the cell cycle is suggestive of post-translational modifications such as phosphorylation. In our early report, GW182 was shown to be phosphorylated when HeLa cells were cultured in radiolabeled ortho-phosphate (Eystathioy et al., 2002a).

Expression of GWB and GW182 are elevated in proliferating versus quiescent cells

Mouse 3T3 cells were synchronized by serum starvation as described in the Materials and Methods. More than five percent of quiescent cells, showed PCNA staining. After serum starvation (Fig. 7A, 0 hour), little or no GW182 staining was detected. At 3 and 6 hours, smaller discrete GWBs (arrows) were observed beginning at 3 and 6 hours after refeeding. Larger and more numerous GWBs were observed at subsequent time points (Fig. 7A). The increased expression of GW182 was confirmed by western blot analysis, which demonstrated an increasing abundance of GW182 in cells after refeeding compared to quiescent cells (Fig. 7B).

As an independent method to evaluate the expression of GW182 and GWBs in proliferating versus quiescent cells, we used ConA stimulation of resting mouse splenocytes or isolated T cells as the test system. IIF analysis showed that GWBs were observed in ConA-treated splenocytes after 3 or 4 days but not in the untreated cells (data not shown). Isolated mouse T cells were used to repeat the ConA stimulation experiment as shown in Fig. 8. Cells treated with ConA had an abundance of GWBs after 3 days (Fig. 8C) in contrast to

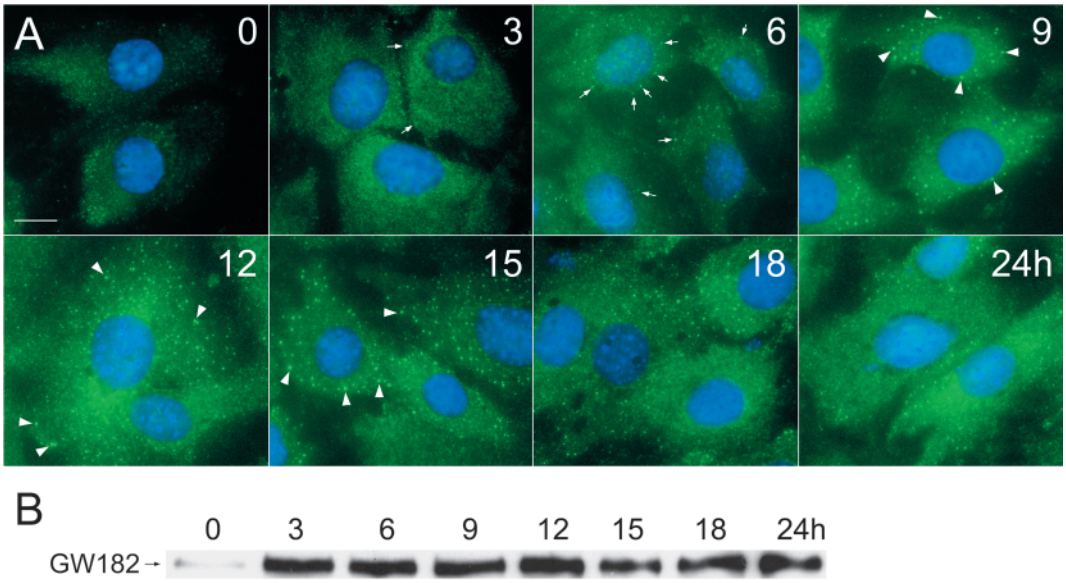

Fig. 7. Increased expression of GWBs and GW182 in proliferating 3T3 cells after release from serum starvation. (A) Cells were analyzed by IIF at different time points after refeeding, as indicated. At 0 hours, there was little or no staining from human anti-GW182 serum. Smaller discrete GWBs (arrows) were observed beginning at 3 and 6 hours after refeeding. Larger and more numerous GWBs were observed at the subsequent time points (arrowheads). Scale bar: 10 μm. (B) Cells were harvested at different time points and supernatant fractions were separated in a 5% gel by SDS-PAGE and transferred to a nitrocellulose membrane that was later probed with a human anti-GW182 serum.

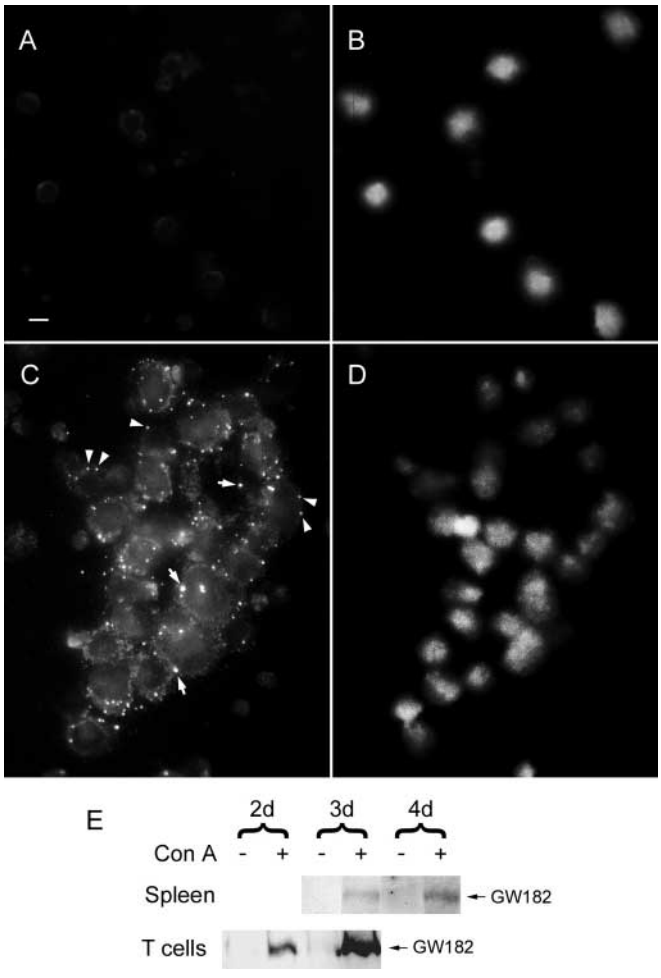

untreated cells (Fig. 8A). Both small and large GWBs were observed in the stimulated cells. Cell extracts from treated and untreated splenocytes and isolated T cells were analyzed by western blot (Fig. 8E). GW182 was observed only in ConA-treated and not in untreated cells (Fig. 8E). The western blot data on GW182 confirmed the observation that ConA-treated isolated T cells had more GWBs at days 2 and 3 compared to ConA-treated splenocytes at days 3 and 4, suggesting that non-T cells in the splenocyte preparation do not express GW182. These data are consistent with the serum starvation data showing that, in comparison to quiescent cells, the expression of GW182 and GWBs is elevated in proliferating cells.

GWBs are dynamic structures capable of fusion

Based on the observation that the number and size of GWBs vary during the cell cycle, the dynamics of these structures is interesting since it may be possible to detect fusion of GWBs. The GFP-GW182 construct (Eystathioy et al., 2002a) was transiently transfected into HEp-2 cells, and live cells were examined ~15 hours post-transfection. Serial sectional images

Fig. 8. Enhanced expression of GW182 in proliferating mouse splenocytes and isolated T cells. Isolated mouse spleen cells or purified T cells were cultured in vitro either in the presence or absence of 5μg/ml ConA for 2 to 4 days. (A-D) Representative anti-GW182 IIF images of isolated T cells from day 3. Cells treated with ConA (C) showed cell aggregation and abundant small (arrowheads) and large (arrows) GWBs. Untreated cells were negative for GW182 (A). (B,D) DAPI counterstaining of the cell nuclei shown in A and C, respectively. Scale bar: 10 μm. (E) Western blot comparison of GW182 expression in cells treated with or without ConA.

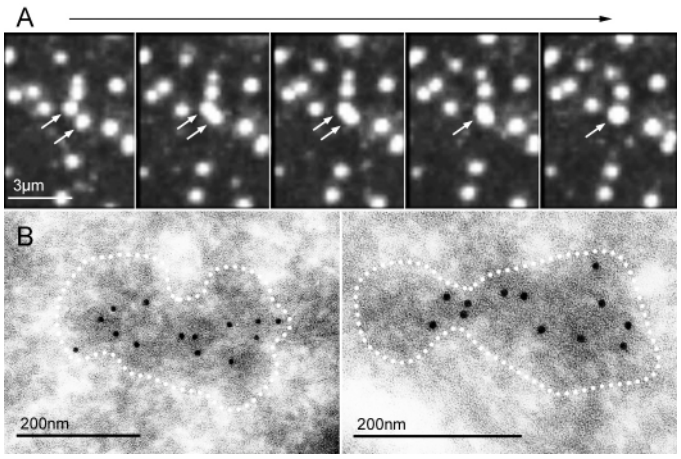

Fig. 9. Fusion of GWBs. (A) A continuous sequence of live cell images showing the fusion of two GFP-labeled GWBs into one (arrows) in a HEp-2 cell transfected with a plasmid construct expressing a GFP-GW182 fusion protein. Original magnification ×1,500. (See also movie 2 in supplementary material.)
(B) ImmunoEM images of protein A-gold-labeled cytoplasmic structures that may be GWBs undergoing fusion (or division). Dotted lines encircle the potential GWBs undergoing fusion similar to the type observed in A.

were captured every 30 seconds up to 1 hour, and 3-D reconstruction was generated with the SoftWoRx deconvolution software. A short video showing the dynamic movement of GWBs in real time can be seen in Movie 1, in supplementary material). The single transfected cell imaged in the video shows primarily back and forth movement of GWBs restricted to the cytoplasm. Fig. 9A shows the composite of five serial images of another transfected cell and documents the ability of two smaller GWBs to fuse together to form one large GWB (arrows). Note that in the last image this large GWB (arrow) was rotated 90 degrees to show that this GWB was truly one single GWB and not merely overlapping GWBs (see also Movie 2, in supplementary material).

In reviewing many IEM images of asynchronous cells labeled with human anti-GW182 antibody and protein A-gold as shown in Fig. 2, images of labeled cytoplasmic structures that might be GWBs undergoing fusion (or division) were noted. Fig. 9B shows two such images that may lend support for the fusion observed by light microscopy, as described above.

siRNA targeting GW182 disrupt GWBs

The two GW182 shRNA plasmids constructed to target GW182 nucleotide position 721 (p721) and 1570 (p1570) were confirmed by DNA sequencing. In an initial experiment, it was shown that p721 abrogated GWBs in transfected cells, whereas the vector pSHAG alone and p1570 did not appear to affect GWBs. These experiments were performed with GFP as a marker for transfected cells and the reduction of GWB staining was observed at 72 hours after transfection. Fig. 10 shows that GWBs were detected in non-transfected cells (arrows, Fig. 10Ai,v) and cells transfected with pSHAG vector control (arrowheads, Fig. 10Av,viii), but were absent in cells with the siRNA construct (arrowheads, Fig. 10Ai,iv). The human anti-GW182 serum IC6 used in this experiment is known to have additional nuclear envelope antibodies (Ou et al., 2004) and was selected to demonstrate the specific siRNA effect of p721 in knockdown of GW182 and GWB expression. Our data indicated that GWBs apparently disappeared in cells co-tansfected with phrGFP and p721 while the staining of the nuclear envelope was not affected in transfected cells. Cells stained with rabbit anti-LSm4 antibodies often give strong nucleoplasmic staining because LSm4 is also a component of the LSm2-8 complex, which is associated with U6 snRNA in the nucleus (He and Parker, 2000). The cytoplasmic GWB staining of LSm4 occurs because LSm4 is a component of the LSm1-7 complex, which has been associated with mRNA degradation (He and Parker, 2000). Note that p721-induced GW182 knockdown in transfected cells did not affect nuclear LSm4 (anti-LSm4, Fig. 10Bi,v) and only the cytoplasmic LSm4-stained bodies were affected and no longer observed.

Although the transient transfection of p721 into HeLa cells could disrupt GWBs, we were unable to demonstrate a convincing reduction in the level of GW182 protein using western blot analysis of the lysates from transfected cells. We reasoned that this was due to the low transfection efficiency (~10-20%) of the shRNA plasmid construct in these cells. As a result, we generated HeLa cell lines using cotransfection of pcDNA3.1(+) and p721 with a molar ratio of 1:10 as described in the Materials and Methods. More than 20 clones were screened by western blotting analysis and IIF. Fig. 11 is representative of the screening procedure and demonstrates the technique used to isolate clone 721A9 that was identified as having RNAi-mediated knockdown of GW182 as observed through western blot analysis (Fig. 11A) and IIF studies (Fig. 11B). The GW182 protein levels of clone 721A9 were knocked down compared to the levels of GW182 in HeLa cells and clone 721B9, a clone that did not appear to have the shRNA plasmid construct p721 incorporated into its genome, but did have the pcDNA3.1 plasmid due to its maintained G418 resistance in tissue culture. Similarly, IIF studies further verified the western blotting analysis data and the transient transfection results discussed in Fig. 10. Clone 721A9 had fewer GWBs in comparison to clone 721B9 (Fig. 11B ii and i, respectively) and HeLa cells (data not shown). Interestingly, RNAi-mediated stable inactivation of GW182 (clone 721A9) similarly disrupted the cytoplasmic distribution of LSm4 in comparison to clone 721B9 (Fig. 11B, iv and iii, respectively). The above data further corroborated the results seen in the transient transfection studies and supports the notion that GW182 appears to be involved in the structure/maintenance and/or stability of GWBs.

Discussion

In the present study, we showed that the expression of GWBs varied through the cell cycle in asynchronous cell lines and cells synchronized by double thymidine treatment at early S phase. Large GWBs were detected primarily in late S and G2 cells where levels of CENP-F are known to be highest. IEM analysis showed electron dense immunogold-labeled bodies in the cytoplasm, some of which were located near the nuclear

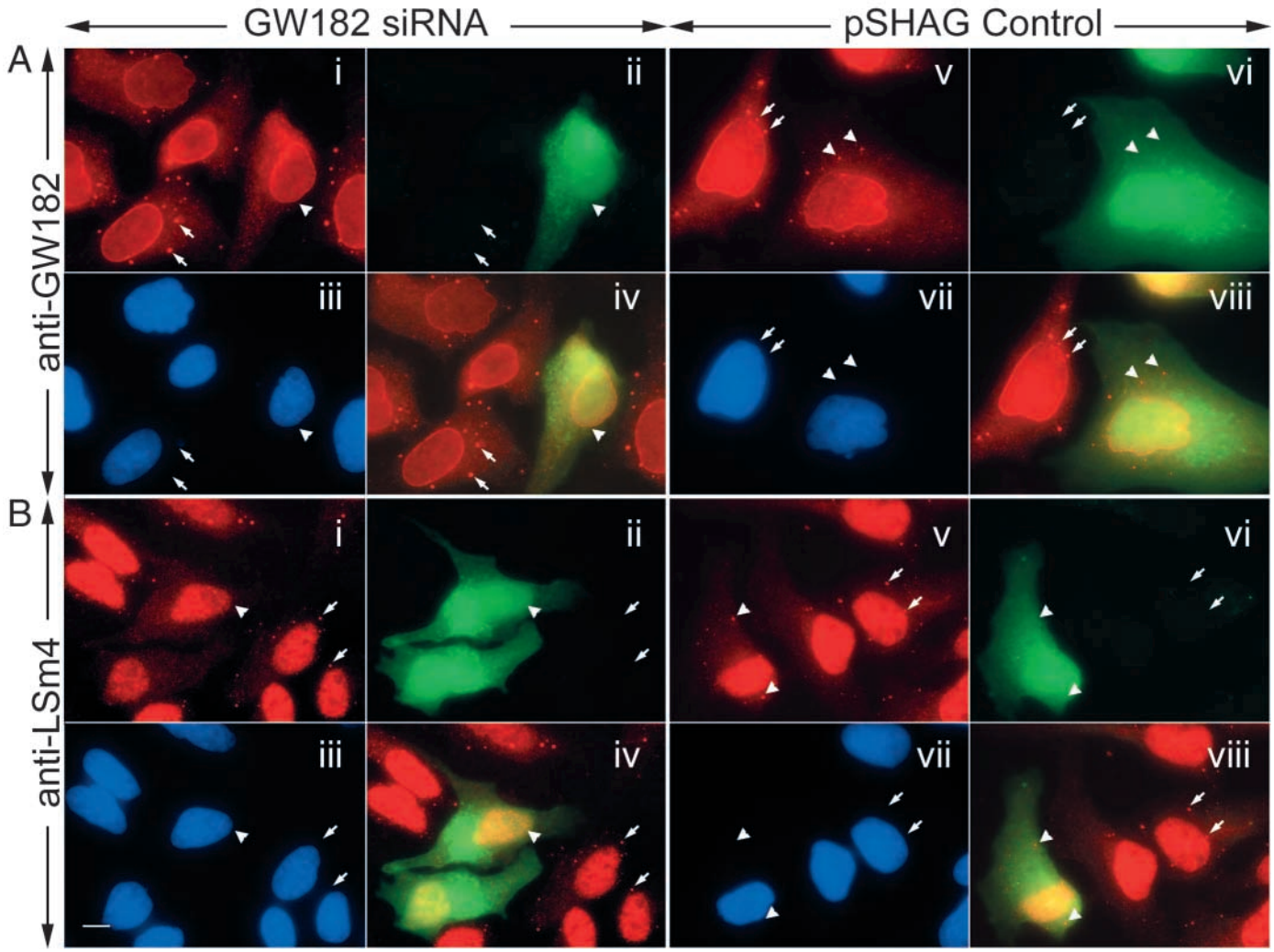

Fig. 10. GW182 is the GWB 'matrix/scaffold' protein as revealed in gene knockdown experiments. GW182 (A) and LSm4 (B) in GWBs are detected by staining with respective antibodies and Alexa Fluor 555-conjugated secondary antibody (red; i,v). GW182 siRNA construct-transfected cells are marked by green fluorescent protein, via cotransfection with phrGFP, which is detected both in the nucleus and cytoplasm (ii,vi). GWBs are detected in non-transfected cells (arrows, i,v) and cells transfected with pSHAG vector control (arrowheads, v,viii) but are absent in cells with the siRNA construct (arrowheads, i,iv). (iv,viii) Merged images. Nuclei are counterstained with DAPI (iii,vii). Scale bar: 10 μm.

envelope. Substantially smaller cytoplasmic structures were detected in mitotic cells. Like many intracellular structures, including the nucleus, nucleolus, Cajal bodies and Golgi complex, GWBs appear to disassemble prior to mitosis and reassemble after cell division. Using two different systems of cell proliferation, it was shown that GWBs and GW182 expression are low in quiescent cells but became elevated in proliferating cells. The elevation in GW182 in proliferating cells is consistent with our observation that some breast cancer tissues have higher levels of immunoreactive GW182 as demonstrated by staining with a murine monoclonal anti-GW182 antibody (Eystathioy et al., 2003a). Using a GFP-tagged GW182 fragment, GWBs were observed as dynamic structures capable of fusing with each other. Lastly, siRNA GW182 knockdown studies strongly suggest that GW182 is a critical component of GWBs and the absence of GW182 inhibits the localization of LSm4 to this cytoplasmic compartment.

GWBs are dynamic sites for mRNA degradation/regulation

Recent reports have indicated that certain mRNAs and mRNA-processing molecules are localized in distinct cytoplasmic foci (Tharun and Parker, 2001; Van Dijk et al., 2002; Eystathioy et al., 2003c). In our initial report, GWBs were considered potential sites for mRNA storage, based in part on the ability of GW182 to co-precipitate with a subset of mRNAs (Eystathioy et al., 2002a). More recently, we used antibodies to hLSm4 and hDcp1 to show that both of these markers of an mRNA degradation pathway localize to the same structures as GW182 (Eystathioy et al., 2003c). Thus, GWBs are probably the mammalian counterparts of P bodies (processing bodies), which were described recently in yeast as discrete cytoplasmic foci containing LSm complexes and Dcp proteins, and were postulated to be intracellular sites for the major pathway of eukaryotic mRNA turnover that begins with deadenylation, followed by decapping and 5′ to 3′

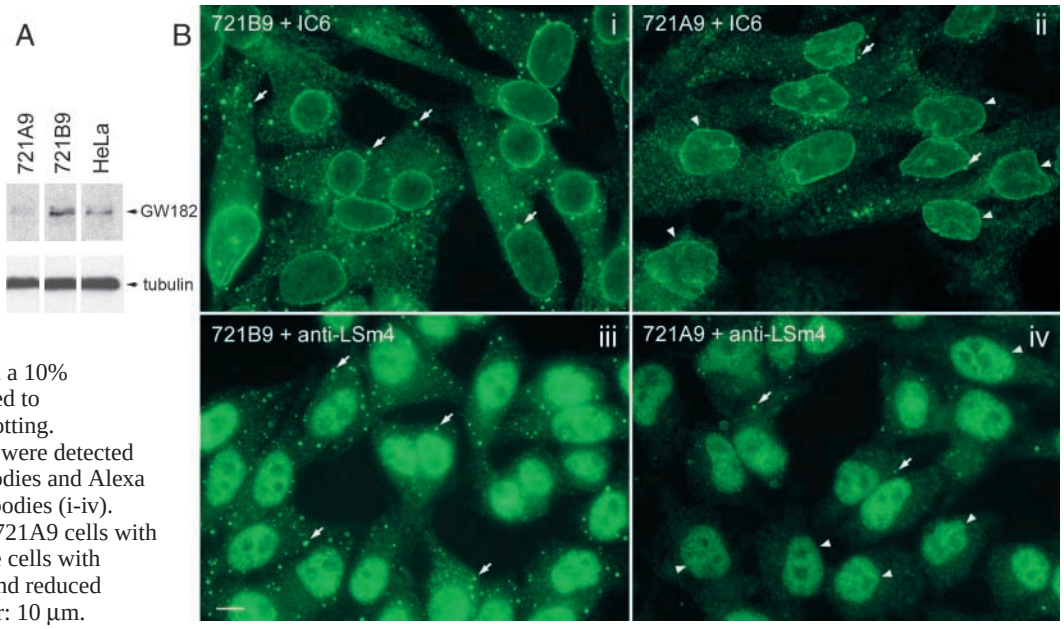

Fig. 11. HeLa cells selected for GW182 gene knockdown demonstrated a reduction in GW182 protein levels and few or no GWBs. (A) Western blot analysis of GW182 expression using the index human anti-GW182 serum in GW182-knockdown cells (721A9), control selected cells (721B9), and control untreated HeLa cells. Tubulin antibody was used to check for equal loading of samples. Cell lysates were run on a 10% polyacrylamide gel and transferred to nitrocellulose prior to immunoblotting. (B) GW182 and LSm4 in GWBs were detected by staining with respective antibodies and Alexa Fluor-conjugated secondary antibodies (i-iv). Arrowheads in ii and iv indicate 721A9 cells with few or no GWBs; arrows indicate cells with normal GWB expression (i,iii), and reduced GWB expression (ii,iv). Scale bar: 10 μm.

exonucleolytic decay (Sheth and Parker, 2003). It has been suggested that mRNA entry into and exit from these cytoplasmic foci could provide a new means for the control of these transcripts, and by extension, gene expression (Wickens and Goldstrohm, 2003). Our study using GFP-GW182 shows an additional dimension of the dynamic nature of these foci, which are enriched with mRNA turnover macromolecules and for which GW182 is an independent marker. It would be interesting to further measure the dynamics of GWBs using mRNA probes.

Ultrastructure of GWBs

This study clearly showed that GWBs are not bound by a lipid bilayer membrane. The IEM labeling with protein A-gold facilitated the observation that the majority of GWBs were distinctive electron dense clusters readily recognized at relatively low magnification. At higher magnification, GWBs appeared to be composed of electron dense fibrils or strands, 8-10 nm in diameter, reminiscent of the ultrastructure of the Cajal body (previously also known as the coiled body) (Raska et al., 1991). One difference, is that the Cajal body appears more spherical at the EM level and the ~30 nm strands appear to be larger in diameter than GWBs (Monneron and Bernhard, 1969). The Cajal body could be as much as 1,000 nm in diameter, whereas the largest GWB measured in our study was ~300 nm in diameter. Other than the observation that GWBs were often seen adjacent to the cytoplasmic face of the nuclear envelope at the light microscopy level, association with other cytoplasmic organelles was not observed. This close proximity to the nuclear envelope is interesting because this suggests that GW182 may be recruiting maturing mRNA as it is exported to the cytoplasm and thus GWBs may serve as potential storage sites as proposed in our earlier report (Eystathioy et al., 2002a). However, in the present study no GWBs were observed directly adjacent to any well defined nuclear pore structures. Further studies are needed to locate GW182 and candidate nuclear envelope proteins to determine if there are yet to be defined molecular interactions.

Suppression of GW182 gene expression by RNA interference disrupts GWBs in HeLa cells

Our GW182 siRNA knockdown data suggest that GW182 is a critical component of GWBs. Although there are two additional GW182-like gene products detected in the human genome database (our unpublished data) and our preliminary data showed that these two GW182-like proteins could be localized to GWBs in transfection studies, our siRNA gene knockdown data showed that the reduction of GW182 led to the disappearance of GWBs as defined by absence of staining by anti-GW182 antibody and disappearance of cytoplasmic, but not nuclear, staining by anti-LSm4 antibodies. We hypothesize that GW182 may act as a matrix or scaffold on which GWBs are assembled. A reduction of the level of GW182 may lead to the disruption or disassembly of GWBs. The IEM data support this working hypothesis because all of the gold particles have been detected on the 8-10 nm diameter fibrils/strands, which may be composed of GW182 protein RNA complexes. The unusual GW repeats spaced throughout the amino-terminal half of GW182 may provide the means for protein-protein interaction and its ability to serve as a GWB matrix. Further work is needed to determine whether these structural features can account for some of our observations.

We acknowledge the technical assistance of Messrs John C. Hamel and Brian Smith. Dr Lei Xiao, Department of Anatomy and Cell Biology, University of Florida, is acknowledged for her guidance in designing and selecting the stable cell lines. This work was supported in part by the Canadian Institutes for Health Research Grant MOP-38034 and the National Institutes of Health Grants AI47859 and AI39645. M.J.F. holds the Arthritis Society Chair at the University of Calgary, Canada.

Reference

Andrade, L. E. C., Tan, E. M. and Chan, E. K. L. (1993). Immunocytochemical analysis of the coiled body in the cell cycle and during cell proliferation. *Proc. Natl. Acad. Sci. USA* **90**, 1947-1951.

Bootsma, D., Budke, L. and Vos, O. (1964). Studies on synchronous division of tissue culture cells initiated by excess thymidine. *Exp. Cell Res.* **33**, 301-309.

Bouveret, E., Rigaut, G., Shevchenko, A., Wilm, M. and Séraphin, B. (2000). A Sm-like protein complex that participates in mRNA degradation. *EMBO J.* **19**, 1661-1671.

Bravo, R. and Macdonald-Bravo, H. (1987). Existence of two populations of cyclin/proliferating cell nuclear antigen during the cell cycle: association with DNA replication sites. *J. Cell Biol.* **105**, 1549-1554.

Casiano, C. A., Landberg, G., Ochs, R. L. and Tan, E. M. (1993). Autoantibodies to a novel cell cycle-regulated protein that accumulates in the nuclear matrix during S phase and is localized in the kinetochores and spindle midzone during mitosis. *J. Cell Sci.* **106**, 1045-1056.

Casiano, C. A., Humbel, R. L., Peebles, C. L., Covini, G. and Tan, E. M. (1995). Autoimmunity to the cell cycle-dependent centromere protein p330d/CENP-F in disorders associated with cell proliferation. *J. Autoimmun.* **8**, 575-586.

Couttet, P., Fromont-Racine, M., Steel, D., Pictet, R. and Grange, T. (1997). Messenger RNA deadenylylation precedes decapping in mammalian cells. *Proc. Natl. Acad. Sci. USA* **94**, 5628-5633.

Dunckley, T. and Parker, R. (1999). The DCP2 protein is required for mRNA decapping in Saccharomyces cerevisiae and contains a functional MutT motif. *EMBO J.* **18**, 5411-5422.

Dunckley, T. and Parker, R. (2001). Yeast mRNA decapping enzyme. *Methods Enzymol.* **342**, 226-233.

Eystathioy, T., Chan, E. K. L., Tenenbaum, S. A., Keene, J. D., Griffith, K. and Fritzler, M. J. (2002a). A phosphorylated cytoplasmic autoantigen, GW182, associates with a unique population of human mRNAs within novel cytoplasmic speckles. *Mol. Biol. Cell* **13**, 1338-1351.

Eystathioy, T., Peebles, C. L., Hamel, J. C., Vaughn, J. H. and Chan, E. K. L. (2002b). Autoantibody to hLSm4 and the heptameric LSm complex in anti-Sm sera. *Arthritis Rheum.* **46**, 726-734.

Eystathioy, T., Chan, E. K. L., Mahler, M., Luft, L. M., Fritzler, M. L. and Fritzler, M. J. (2003a). A panel of monoclonal antibodies to cytoplasmic GW bodies and the mRNA binding protein GW182. *Hybrid. Hybridomics* **22**, 79-86.

Eystathioy, T., Chan, E. K. L., Takeuchi, K., Mahler, M., Luft, L. M., Zochodne, D. W. and Fritzler, M. J. (2003b). Clinical and serological associations of autoantibodies to GW bodies and a novel cytoplasmic autoantigen GW182. *J. Mol. Med.* **81**, 811-818.

Eystathioy, T., Jakymiw, A., Chan, E. K. L., Séraphin, B., Cougot, N. and Fritzler, M. J. (2003c). The GW182 protein colocalizes with mRNA degradation associated proteins hDcp1 and hLSm4 in cytoplasmic GW bodies. *RNA* **9**, 1171-1173.

Gao, M., Wilusz, C. J., Peltz, S. W. and Wilusz, J. (2001). A novel mRNA-decapping activity in HeLa cytoplasmic extracts is regulated by AU-rich elements. *EMBO J.* **20**, 1134-1143.

He, W. and Parker, R. (2000). Functions of Lsm proteins in mRNA degradation and splicing. *Curr. Opin. Cell Biol.* **12**, 346-350.

Ingelfinger, D., Arndt-Jovin, D. J., Luhrmann, R. and Achsel, T. (2002). The human LSm1-7 proteins colocalize with the mRNA-degrading enzymes Dcp1/2 and Xrnl in distinct cytoplasmic foci. *RNA* **8**, 1489-1501.

Keene, J. D. (2003). Posttranscriptional generation of macromolecular complexes. *Mol. Cell* **12**, 1347-1349.

Liao, H., Winkfein, R. J., Mack, G., Rattner, J. B. and Yen, T. J. (1995). CENP-F is a protein of the nuclear matrix that assembles onto kinetochores at late G2 and is rapidly degraded after mitosis. *J. Cell Biol.* **130**, 507-518.

Linstedt, A. D. and Hauri, H. P. (1993). Giantin, a novel conserved Golgi membrane protein containing a cytoplasmic domain of at least 350 kDa. *Mol. Biol. Cell* **4**, 679-693.

Mishell, B. B. and Shiigi, S. M. (1980). *Methods in Cellular Immunology*, pp. 182-185. New York, NY: W. H. Freeman and Company.

Monneron, A. and Bernhard, W. (1969). Fine structural organization of the interphase nucleus in some mammalian cells. *J. Ultrastruct. Res.* **27**, 266-288.

Oliver, B., Parisi, M. and Clark, D. (2002). Gene expression neighborhoods. *J. Biol.* **1**, 4.

Ou, Y., Enarson, P., Rattner, J. B., Barr, S. G. and Fritzler, M. J. (2004). The nuclear pore complex protein Tpr is a common autoantigen in sera that demonstrate nuclear envelope staining by indirect immunofluorescence. *Clin. Exp. Immunol.* **136**, 379-387.

Paddison, P. J., Caudy, A. A., Bernstein, E., Hannon, G. J. and Conklin, D. S. (2002). Short hairpin RNAs (shRNAs) induce sequence-specific silencing in mammalian cells. *Genes Dev.* **16**, 948-958.

Raposo, G., Kleijmeer, M. J., Posthuma, G., Slot, J. W. and Geuze, H. J. (1996). Immunogold labeling of ultrathin cryosections: application in immunology. In *Weir's Handbook of Experimental Immunology* (ed. D. M. Weir), pp. 1-11. New York, NY: Blackwell Publishers.

Raska, I., Andrade, L. E. C., Ochs, R., Chan, E. K. L., Chang, C. M., Roos, G. and Tan, E. M. (1991). Immunological and ultrastructural studies of the nuclear coiled body with autoimmune antibodies. *Exp. Cell Res.* **195**, 27-37.

Rattner, J. B., Rao, A., Fritzler, M. J., Valencia, D. W. and Yen, T. J. (1993). CENP-F is a .ca 400 kDa kinetochore protein that exhibits a cell-cycle dependent localization. *Cell Motil. Cytoskeleton* **26**, 214-226.

Reimer, G., Pollard, K. M., Penning, C. A., Ochs, R. L., Lischwe, M. A., Busch, H. and Tan, E. M. (1987). Monoclonal autoantibody from a (New Zealand black x New Zealand white) F1 mouse and some human scleroderma sera target an Mr 34,000 nucleolar protein of the U3 RNP particle. *Arthritis Rheum.* **30**, 793-800.

Sheth, U. and Parker, R. (2003). Decapping and decay of messenger RNA occur in cytoplasmic processing bodies. *Science* **300**, 805-808.

Spellman, P. T. and Rubin, G. M. (2002). Evidence for large domains of similarly expressed genes in the Drosophila genome. *J. Biol.* **1**, 5.

Takasaki, Y., Fishwild, D. and Tan, E. M. (1984). Characterization of proliferating cell nuclear antigen recognized by autoantibodies in lupus sera. *J. Exp. Med.* **159**, 981-992.

Tharun, S. and Parker, R. (2001). Targeting an mRNA for decapping: displacement of translation factors and association of the Lsm1p-7p complex on deadenylated yeast mRNAs. *Mol. Cell* **8**, 1075-1083.

Tharun, S., He, W., Mayes, A. E., Lennertz, P., Beggs, J. D. and Parker, R. (2000). Yeast Sm-like proteins function in mRNA decapping and decay. *Nature* **404**, 515-518.

Van Dijk, E., Cougot, N., Meyer, S., Babajko, S., Wahle, E. and Séraphin, B. (2002). Human Dcp2: a catalytically active mRNA decapping enzyme located in specific cytoplasmic structures. *EMBO J.* **21**, 6915-6924.

Wickens, M. and Goldstrohm, A. (2003). Molecular biology. A place to die, a place to sleep. *Science* **300**, 753-755.